PARAMETRIC STUDY OF NON-EVAPORATIVE SPRAY COOLING ON ALUMINUM PLATE: Simulation and Analysis

by

Abdessalam OTMANI[a*] and Hocine MZAD[b]

[a]Laboratory of Industrial Mechanics, Badji Mokhtar University of Annaba, Annaba, Algeria
[b]Department of Mechanical Engineering, Badji Mokhtar University of Annaba, Annaba, Algeria

Original scientific paper
https://doi.org/10.2298/TSCI19S4393O

As the behavior of the spray cooling parameters, during cooling without phase change, is rarely considered and there are only little investigations on that matter, this work is focused on the influence of the parameters involved in water spraying cooling process of an aluminum plate at a temperature of 92 °C. A detailed study of the effects of mass-flow rate, fluid pressure and the nozzle height above the hot plate was achieved using the version 5.2 of the COMSOL Multiphysics code. First of all, the flow rate was varied from 0.497 up to 1 L/min. Then, the inlet pressure varied from 0.7 to 2.1 bars. The influence of nozzle-to-target distance is also tested since the simulations were carried out in a wide height range (100 to 505 mm). The effect of the studied parameters on the temperature, total internal energy, convective heat flux, Reynolds number, spray distribution and velocity was investigated.

Key words: *nozzle, dispersion, impinging flow, modeling, simulation, heat dissipation*

Introduction

Spray cooling is a technology of increasing interest for several domains (energy, automotive, aerospace, electronics, metallurgy, *etc*.) and it require a precise definition of the cooling parameters. The thermal performance during spray injection of liquid onto surfaces is normally represented by the associated heat transfer coefficient or the Nusselt number, which is a measure of the cooling rate due to forced convection. Characterization of the heat transfer coefficient is important for determining the required cooling capacity and corresponding internal properties of the product. For this reason, a vast amount of work has been devoted to parameterize or model the heat transfer coefficient during spray cooling in different flow regimes [1, 2]. Thibaud *et al.* [3] calculated and extrapolated the heat transfer coefficient distributions for various spray quenching parameters (water volume flow and air pressure) as well as quenching profiles with aluminum and a steel plate. Using the calculated and implemented heat transfer coefficients, several quenching scenarios aiming at cooling down a 200 °C, 1.5 × 0.3 m² thin aluminum plate below 50 °C in less than 25 seconds has been evaluated. Mudawar [4] realized an interesting study for optimizing spray quenching of aluminum extrusion, forging, or continuous casting. A numerical example was described to demonstrate how controlled

* Corresponding author, e-mail: abdessalam.othmani@univ-annaba.org

spray cooling of products containing sections of differing thicknesses significantly reduces thermal gradients.

A correlation was established for the quantification of water jet dispersion on the totality of a plane surface in the function of the spray nozzle dimensions and hydrodynamic parameters. Subsequently, numerical simulations based on the previous experimental results were conducted to investigate the effect of the water-spray characteristics on the heat transfer mechanisms involved during cooling of steel plates at high temperatures [5, 6]. A model to predict the heat and mass transfer in spray cooling was presented with consideration of droplet-film impaction, film formation, film motion, bubble boiling, droplet-bubble interaction, bulk air convection and radiation [7]. If multiple nozzles are used in a conveyorized application, the overlapping liquid distribution pattern of the nozzles needs to be considered because the process may depend strongly on the relative local volume flux of the spray. In order to understand the fluid behavior in the overlap region, a hydrodynamic study was proposed using a FORTRAN programming based on experimental correlations of pulverized water jets [8]. The effects of droplet velocity non-uniformity, Sauter mean diameter distribution non-uniformity, droplet number non-uniformity, and the heating power on the fluid film thickness, fluid film velocity, and surface temperature distribution were investigated, and then the surface temperature non-uniformity correlations in non-boiling regime and nucleate boiling regime were correlated [9]. The heat transfer characteristics of air-water spray impingement cooling of stationary steel plate were experimentally investigated. The controlling parameters taken during the experiments were fluid pressure, water-flow rate, nozzle tip to target distance and mass impingement density. The effects of the controlling parameters on the cooling rates were critically examined during spray impingement cooling [10, 11]. A CFD assessed the potential and performance of evaporative cooling by water spray system with a hollow-cone nozzle configuration [12]. Nizetic *et al.* [13, 14] proposed an alternative cooling technique for photovoltaic (PV) panels that includes a water spray application over panel surfaces. Both sides of the PV panel were cooled simultaneously, to investigate the total water spray cooling effect on the PV panel performance in circumstances of peak solar irradiation levels. Furthermore, it was also possible to decrease panel temperature from an average 54 °C (non-cooled PV panel) to 24 °C in the case of simultaneous front and backside PV panel cooling.

The purpose of this study is to highlight, by simulation under COMSOL Multiphysics, the influence of hydrodynamic parameters, namely the nozzle height, water-flow rate and spraying pressure in order to evaluate the impact of nozzle characteristics and operating conditions on cooling performance of the spray system.

Modelling and simulation

In the simplest case, a single nozzle is employed to distribute liquid in a definite pattern to cover a surface or fill a spatial volume in a prescribed manner. Hydraulic atomizers depend on the internal geometry and liquid pressure alone to produce a desired pattern. The exact definition of the spray characteristics and the specification of the operation parameters are the first two steps to be taken when a spray nozzle is being designed. Using the commercial software COMSOL Multiphysics 5.2 we achieved a specific application, coupled between heat transfer and fluid-flow interface, for the simulation of a cooling process beneath liquid sprayer. The objective is to cool an aluminum 3003-H18 plate, tab. 1, with 6 mm thickness and an area of 1200 mm^2, initially at the temperature of 92 °C. A single BETE WL6 nozzle fixed at the center upon the plate, delivers the simulated water spray in an ambience at atmospheric pressure and a temperature of 20 °C. The nozzle geometry and meshing are shown in

fig. 1.The modelling section is executed in two steps, the fluid-flow model and heat transfer model.

Table 1. Aluminium 3003-H18 Properties

Parameter	Value
Specific heat capacity, C_p	890 [$Jkg^{-1}K^{-1}$]
Density, ρ	2.8 [gcm^{-3}]
Thermal conductivity, k	180 [$Wm^{-1}K^{-1}$]
Thermal expansion coefficient, α	2.3E-5 [K^{-1}]
Melting point, T_m	913 [K]

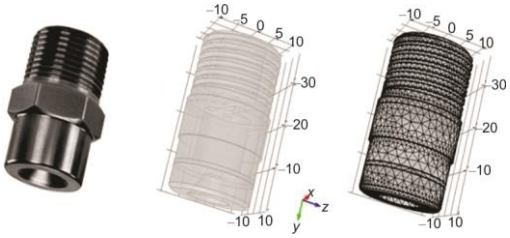

Figure 1. Design and meshing of the nozzle BETE WL6

Fluid-flow model

The resolution of the Navier-Stokes equations was achieved for laminar fluid-flow and stationary regime. The simulation was realized in two steps. The first one is the simulation of the laminar flow around the aluminum plate, inside and outside the nozzle. The obtained results were used in the second step, which is the simulation of the laminar bubbly flow, fig. 2.

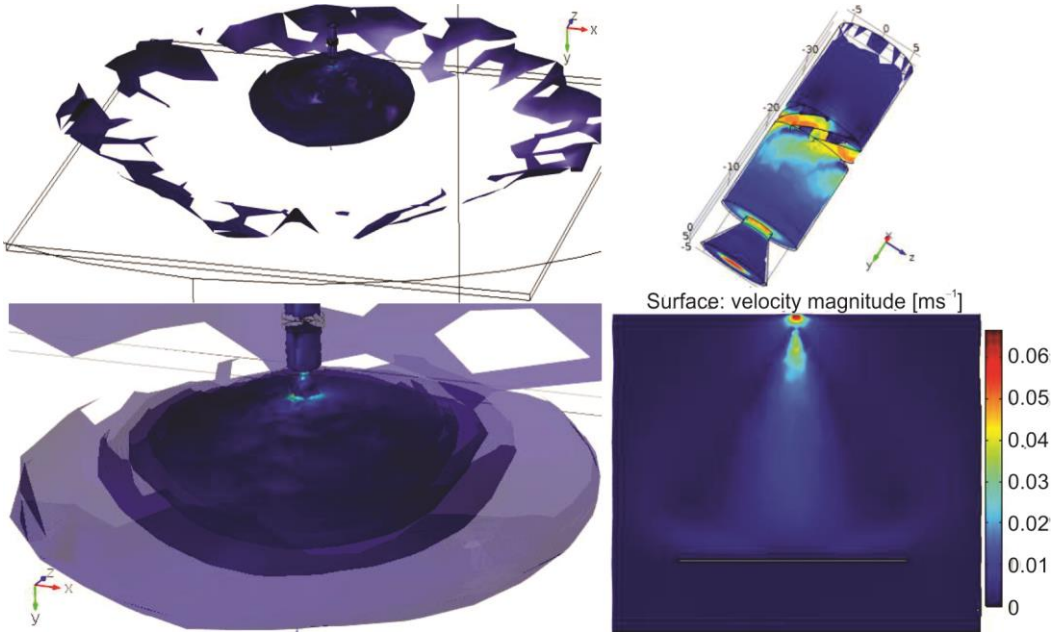

Figure 2. Simulation of the fluid dispersion inside and outside the nozzle (*for colour image see journal web site*)

Using a two-phase Euler-Euler model, a momentum balance equation and a continuity equation describe the dynamics of each phase. As the accuracy of the Euler-Euler method and Euler-Lagrange method depend on the drag force model and there is little investigation on that at supercritical condition [15], the bubbly flow method was used. In fact, it is a simple case of the two-fluid-flow model, relying on the following assumptions.

The gas density is negligible compared to the liquid density; The bubbles motion ($d_b \approx 0.019$ mm) through the liquid is determined by a viscous drag and pressure forces balance; The two phases share the same pressure field. Therefore, a momentum equation is expressed:

$$\phi_l \rho_l \frac{\partial u_l}{\partial t} + \phi_l \rho_l u_l \nabla u_l = -\nabla p + \nabla \left\{ \phi_l (\mu_l + \mu_T) \left[\nabla u_l + \nabla u_l^T - \frac{2}{3} (\nabla u_l) I \right] \right\} + \phi_l \rho_l \mathrm{g} + F \tag{1}$$

and the continuity equation:

$$\frac{\partial}{\partial t} \left(\rho_l \phi_l + \rho_g \phi_g \right) + \nabla \left(\rho_l \phi_l u_l + \rho_g \phi_g u_g \right) = 0 \tag{2}$$

Thus the gas phase transport equation is:

$$\frac{\partial \rho_g \phi_g}{\partial t} + \nabla \left(\phi_g \rho_g u_g \right) = -m_{gl} \tag{3}$$

The gas velocity u_g is the sum of the following velocities:

$$u_g = u_l + u_{\text{slip}} + u_{\text{drift}} \tag{4}$$

The liquid volume fraction is calculated from:

$$\phi_l = 1 - \phi_g \tag{5}$$

The drift velocity expression is:

$$u_{\text{drift}} = -\frac{\tilde{\mu}}{\rho_l} \frac{\nabla \phi_g}{\phi_g} \tag{6}$$

Where is an effective viscosity causing the drift. A combination of previous equations gives:

$$\frac{\partial \rho_g \phi_g}{\partial t} + \nabla \left[\phi_g \rho_g \left(u_l + u_{\text{slip}} \right) \right] = \nabla \left(\frac{\tilde{\mu} \rho_g}{\rho_l} \nabla \phi_g \right) - m_{gl} \tag{7}$$

A diffusive term is introduced in the gas transport equation, eq. (3), which is implemented in the fluid-flow model.

Heat transfer model

The temperature distribution in a 3-D space within the considered solid is described by the equation of the heat conduction:

$$\rho C_p \frac{\partial T}{\partial t} + \rho C_p u \nabla T + \nabla q = 0 \tag{8}$$

where $q = -k\nabla T$

By solving the heat equation, we evaluate the maximum plate temperature variation, the average total internal energy and the average convective heat flux. The convective heat flux variable, C_{flux}, is defined using the internal energy, E:

$$C_{\text{flux}} = \rho u E \tag{9}$$

where $E = C_p T$

The total internal energy is calculated from:

$$E_0 = E + \frac{1}{2}uu \tag{10}$$

There is no liquid evaporation, because the maximum plate temperature is below the water saturation temperature. The initial water supply temperature was 20 °C. The heat transfer in fluid-flow is solved using the equation:

$$\rho C_p \left(\frac{\partial T}{\partial t} + u\nabla T \right) + \nabla \left(q + q_r \right) = Q_p + Q_{Vd} \tag{11}$$

Equation in which:

$$Q_p = \alpha_p T \left(\frac{\partial p}{\partial t} + u\nabla p \right) \tag{12}$$

$$\alpha_p = -\frac{1}{\rho}\frac{\partial \rho}{\partial T} \tag{13}$$

and

$$Q_{Vd} = \tau : \nabla u \tag{14}$$

These terms represents viscous dissipation in the fluid. For the gas density estimation, the model use the ideal gas law, *i. e*. the thermal expansion coefficient $\alpha_p = 1/T$. The grid generation was executed resulting in a free tetrahedral meshing, a finer grid is applied for the nozzle and extra-coarse grid for the aluminum plate and the controlled volume. The mesh information is shown in tab. 2.

Table 2. Free tetrahedral mesh composition

Complete mesh consists of	
Domain elements	41640
Boundary elements	5100
Edge elements	541

Results and discussion

Effect of mass-flow rate

The flow values tested are 0.497, 0.7, and 1 L/min. The results in fig. 3 show a rapid decrease of the plate temperature during the first five minutes. The rest of time there is a very slow decrease of the temperature until t = 60 minute, this is due to the insignificant temperature difference between the plate and the impinging water. To disclose the influence of flow variation on heat transfer, an enlargement, fig. 3, makes it possible to distinguish the flow rate increase effect on the cooling stretch. In fact, the amount of water used plays the same role as in heat exchangers and contributes to the heat evacuation and consequently the plate internal energy decreases, fig. 4.

Convection heat is also influenced by water-spray flow, since we notice a decrease in convective heat flux which is the evident consequence of the simultaneous temperature and internal energy fall, fig. 5.

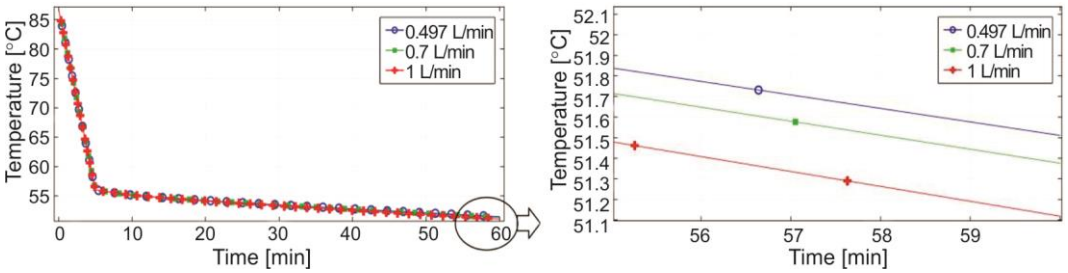

Figure 3. Plate temperature decrease profile under flow rate variation

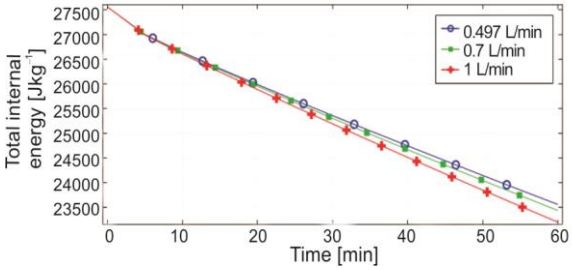

Figure 4. Time evolution of the plate total internal energy with flow rate

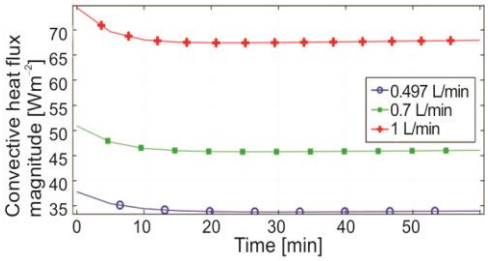

Figure 5. Flow rate effect on temporary heat flux

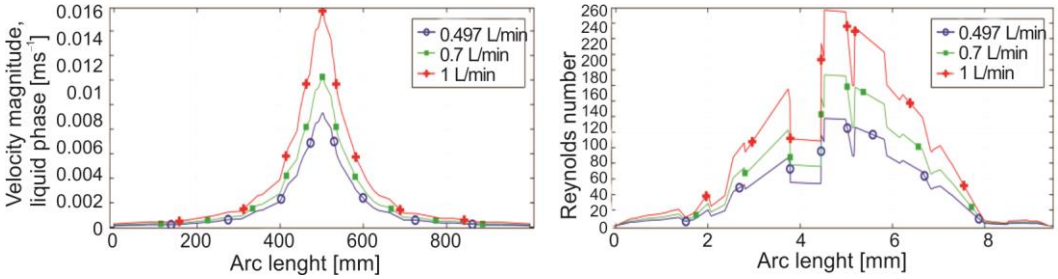

Figure 6. Flow rate effect on spray velocity and Reynolds number, 56.5 mm below the nozzle orifice

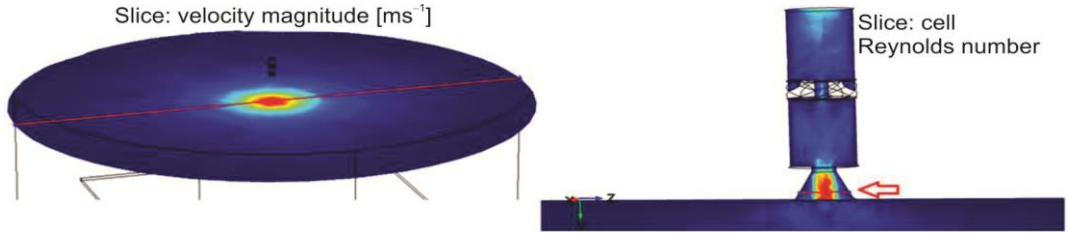

Figure 7. Location of speed and Reynolds number measurement (red lines)
(*for colour image see journal web site*)

The heat dissipation corresponding to a flow-rate of 0.497 L/min is 38 kW/m^2. This value is doubled when the flow goes to 1 L/min, high Reynolds numbers promote forced convection, fig. 6. The spray velocity values are measured on the horizontal median route (red line) at a virtual plan situated at 56.5 mm below the nozzle, fig.7.

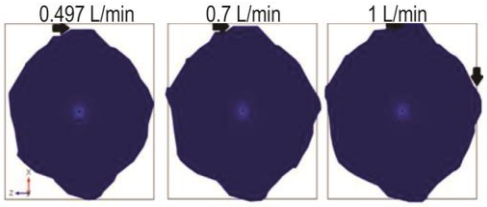

Figure 8. Spray distribution for different flow rates

The covered area by water droplets is a very important factor in spray cooling. In fact, fig. 8, clearly shows that the area covered by the water-spray depends on the initial flow-rate, visibly the area of water dispersion increases with its flow-rate. If we take for example the upper part of the plate, we note that the spray does not cover this area for a flow-rate value of 0.497 L/min, beside the same area is fully covered when the inlet flow is 1 L/min.

Effect of cooling-liquid pressure

The goal in this section is to determine the pressure of optimum cooling among those applied, namely 0.7 bar, 1.9 bar, and 2.1 bar. From the graphical results obtained on figs. 9 and 10, it appears that the optimum cooling pressure is 2.1 bar. In the current context, it is the pressure that offers the best heat transfer resulting in a simultaneous drop of the plate temperature and the total internal energy, their respective values, at t = 5 min, are 53 °C and 24500 J/kg. The decrease in temperature and internal energy is explained by the heat flux released by forced convection with an average value of approximately 900 W/m^2 during the entire cooling period, fig. 11. For example, at P = 0.7 bar corresponds a heat release of 17 W/m^2, which represents a derisory value compared to the 1100 W/m^2 evacuated at the optimal pressure P = 2.1 bar.

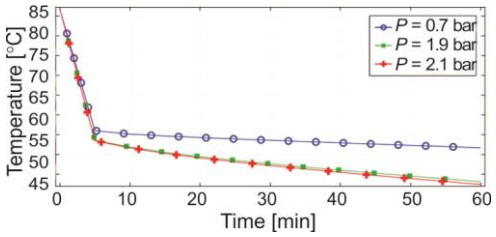

Figure 9. Evolution of plate temperature under spray pressure influence

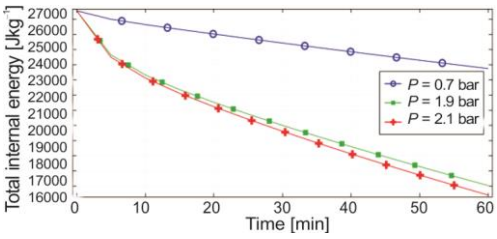

Figure 10. Time evolution of plate total internal energy with spraying pressure

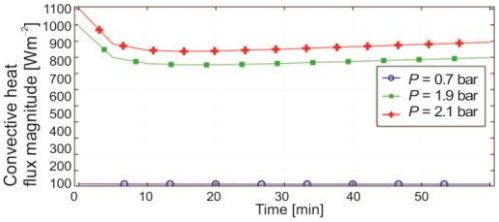

Figure 11. Influence of spraying pressure on convection heat transfer

In fig. 12, it can be seen the evolution of the spray velocity at the level of a virtual horizontal plane along the red median line positioned at 56.5 mm below the nozzle orifice. One note a low spray speed of about 0.004 m/s for P = 0.7 bar, in the same time the velocity exceeds 1 m/s for P = 2.1 bar.

A 300% increase in flow rate causes a fluid velocity increase of the order of 25000%.The surface covered by the spray decreases when the inlet pressure increases, this is the first remark that emerges from the study of the pressure effect on the fluid dispersion, fig. 13. Indeed, if we need to cover a larger surface, we have to reduce the fluid jet pressure. On the other hand, the droplet impingement zone is less important for P = 1.9 and 2.1 bar, but the drops speed is higher, favoring faster cooling.

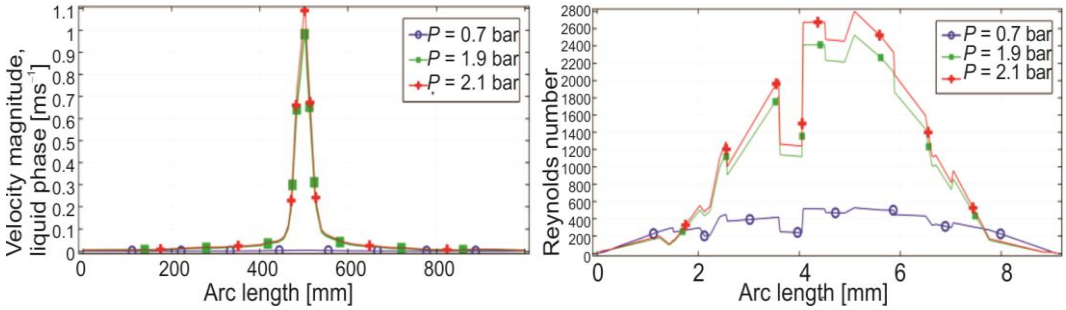

Figure 12. Pressure effect on spray velocity and Reynolds number, 56.5 mm below the nozzle orifice

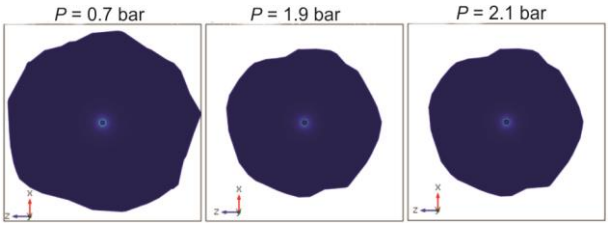

Figure 13. Fluid impingement comparison of different spray pressure

Effect of nozzle height

This section aims to investigate the influence of the nozzle-to-target distance on the cooling spray performance, to be done, we considered four different positions: 100, 191, 330, and 505 mm. The role of this parameter is clearly shown through the figs. 14 and 15 since we note the significant influence of the nozzle position on the plate temperature and its internal energy. In this study, the value H = 505 mm is the optimum height and it is the one that ensures the fastest cooling. The effect of the height also appears on the convection heat flux, fig. 16, indeed for H = 505 mm the significant surface covered by the spray enhances the convection heat transfer. Obviously, the minimum heat flux is recorded for H = 100 mm. Figure 17 displays the spray speed measured at a height of 37 mm above the plate. The drops speed is as much greater as the height decreases. When the nozzle is placed at the optimum height, the spray can cover a wider surface, this is illustrated by the particles tracing shown on fig. 18. A nozzle very close to the plate reduces considerably the impact surface and could affect the surface roughness pattern of the studied material. Finally the choice of the ideal nozzle height for optimal cooling is based on objective analysis of figs. 17 and 18 which will help us to find a compromise between the jet particle speed and the surface covered by the scattered droplets.

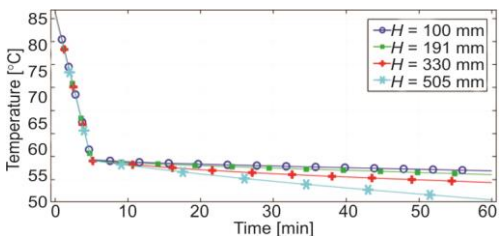

Figure 14. Effect of sprayer height on plate temperature

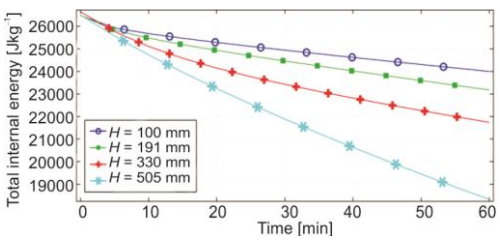

Figure 15. Variation of aluminum plate internal energy with nozzle height

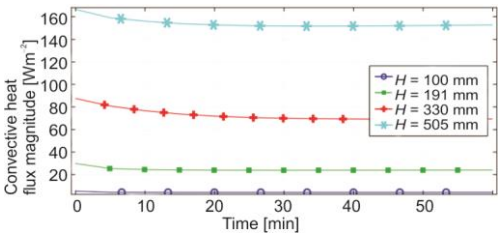

Figure 16. Convection heat flux evolution with nozzle height

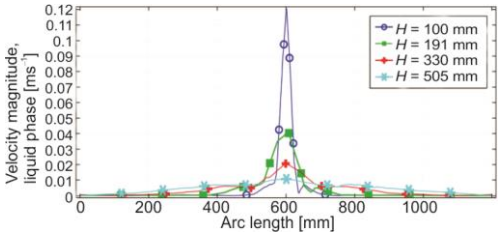

Figure 17. Spray velocity with height variation at 37 mm above the plate

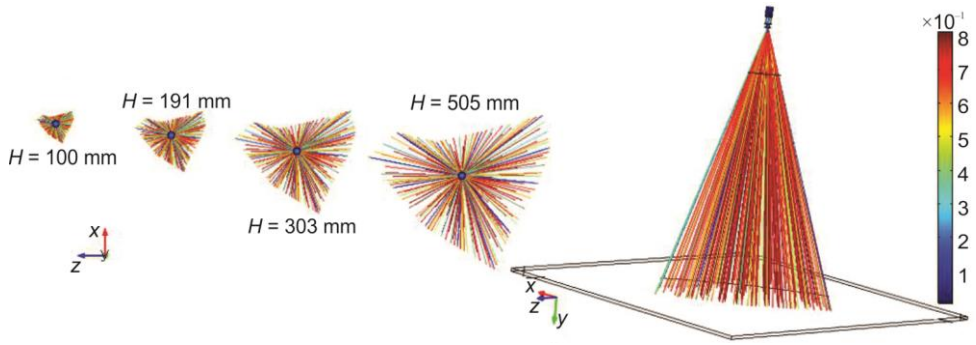

Figure 18.Tracing of 3000 particles for different heights

Sum-up and conclusion

This paper deals with influence of spray cooling process parameters on the thermodynamic behavior of fluid-flow and an aluminum plate at the temperature of 92 °C. Unlike previous studies devoted solely to intensive cooling of highly heated surfaces, the present study makes it possible to observe the evolution of hydrodynamic and thermal parameters during laminar water jet impingement cooling of surface at a temperature below the saturation temperature of the cooling fluid. The results of the simulation discussed in this paper signal the need to provide more insight for parametric analysis during spray cooling process involving the applications in such case of surface temperature (< 100 °C).Increase in electrical efficiency depends primarily on cooling techniques. It is well known that a decrease in the PV panel temperature will lead to an increase in electrical efficiency. Besides, high temperatures reduce the time-life of the PV system. In order to increase the average efficiency in conventional PV panels it is necessary to have more efficient backside thermal dissipation. The backside surface is usually of aluminum made and the analysis presented in this study considering aluminum 3003-H18 cooling allows instantaneously the control and monitoring of PV panels temperature.

Nomenclature

C_{flux} – convective heat flux magnitude, [Wm^{-2}]
C_p – specific heat capacity, [Jkg^{-1}K^{-1}]
E – internal energy, [Jkg^{-1}]
E_0 – total internal energy, [Jkg^{-1}]
F – additional volume force, [Nm^{-3}]
g – gravity acceleration, [ms^{-2}]
I – moment of inertia, [kgm^2]
k – thermal conductivity, [Wm^{-1}K^{-1}]
m_{gl} – gas to liquid mass transfer rate, [kgm^{-3}s^{-1}]
p – pressure, [Pa]
q – conduction heat flux, [Wm^{-2}]

q_r – radiation heat flux, [Wm^{-2}]
R – ideal gas constant, [Jmol^{-1}K^{-1}]
T – temperature,[K]
u – velocity, [ms^{-1}]
u_l – liquid velocity,[ms^{-1}]
u_{slip} – relative velocity, [ms^{-1}]
u_{drift} – drift velocity, [ms^{-1}]

Greek symbols

α_p – coefficient of thermal expansion, [K^{-1}]
ϕ – phase volume fraction, [m^{3}m^{-3}]
ρ – density, [kgm^{-3}]
μ_l – liquid dynamic viscosity, [Pas]
μ_T – turbulent viscosity, [Pas]
$\tilde{\mu}$ – effective viscosity causing the drift, [Pas]

Subscripts

g – gas
l – liquid

References

[1] Webb, B. W., Ma, C. F., Single-Phase Liquid Jet Impingement Heat Transfer, *Advances in Heat Transfer.*, *26* (1995), 17, pp. 105-217
[2] Kim, J., Spray Cooling Heat Transfer: The State of the Art, *International Journal of Heat and Fluid-Flow*, *28* (2007), 4, pp. 753-767
[3] Thibaud, B., *et al*., Characterization of Spray Nozzles for Quenching of Metal Components, *Proceedings*, 26th ILASS Europe, ACASS, Bremen, Germany, 2014, Vol. 54, pp. 763-769
[4] Mudawar, I.,Optimization of Spray Quenching for Aluminum Extrusion, Forging, Orcontinuous Casting, *J. Heat Treat.*, *7* (1989), 1, pp. 9-18
[5] Tebbal, M., Mzad, H., An Hydrodynamic Study of a Water Jet Dispersion Beneath Liquid Sprayers, *Forsch. Ingenieurwes.*, *68* (2004), 3, pp. 126-132
[6] Mzad, H., Tebbal, M., Thermal Diagnostics of Highly Heated Surfaces Using Water-Spray Cooling, *Heat Mass Transfer.*, *45* (2009), Jan., pp. 287-295
[7] Zhao, R., *et al*., Study on Heat Transfer Performance of Spray Cooling: Model and Analysis, *Heat Mass Transfer.*, *46*, (2010), 8, pp. 821-829
[8] Mzad, H., Elguerri, M., Simulation of Twin Overlapping Sprays Underneath Hydraulic Atomizers: Influence of Spray Hydrodynamic Parameters, *Atomization and Sprays.*, *22* (2012), 5, pp. 447-460
[9] Cheng, W. L., *et al*., Theoretical Investigation on the Mechanism of Surface Temperature Non-Uniformity Formation in Spray Cooling, *Int. J. Heat Mass Transfer.*, *55* (2012), 19-20, pp. 5357-5366
[10] Mishra, P. C., *et al*., Effect of Controlling Parameters on Heat Transfer During Spray Impingement Cooling of Steel Plate, *American J. Eng. Res.*, *2* (2013), 9, pp. 8-16
[11] Mzad, H., Rabia, K., Effect of Spraying Pressure on Spray Cooling Enhancement of Beryllium-Copper Alloy Plate, *Procedia Engineering.*, *157* (2016), Dec., pp. 106-113
[12] Montazeri, H., *et al*., Evaporative Cooling by Water Spray Systems: CFD Simulation, Experimental Validation and Sensitivity Analysis, *Build and Env.*, *83* (2015), Jan., pp. 129-141
[13] Nizetic, S., *et al*., Water Spray Cooling Technique Applied on a Photovoltaic Panel: The Performance Response, *Energy Conversion and Management*., *108* (2016), Jan., pp. 287-296
[14] Nizetic, S., *et al*., Experimental and Numerical Investigation of a Backside Convective Cooling Mechanism on Photovoltaic Panels, *Energy.*, *111* (2016), C, pp. 211-225
[15] Wu, Z.-Q., *et al*., Investigation on Drag Coefficient of Supercritical Water Cross-Flow Past Cylinder Biomass Particel at Low Reynolds Number, *Thermal science.*, *22* (2018), Suppl. 2, pp. S383-S389

Paper submitted: March 12, 2019
Paper revised: May 1, 2019
Paper accepted: May 21, 2019